EUSIPCO 2013 1569743613

OPTIMAL WAVEFORMS FOR COMPRESSIVE SENSING RADAR

Lyubomir Zegov[†] *, Radmila Pribić*[*], *Geert Leus*[†]

[†] Delft University of Technology, Delft, The Netherlands
[*]Sensors Advanced Developments, Thales Nederland, Delft, The Netherlands

ABSTRACT

The performance of conventional radar is foreseen to be improved by the implementation of compressive sensing (CS). CS is based on the assumptions of sparsity and incoherence. Here we connect the incoherence of the sensing matrix and the autocorrelation of a radar waveform, and use them as a measure for the design of an optimal waveform in CS based radar. We demonstrate the performance of the waveforms through both matched filtering and sparse signal recovery.

Index Terms— radar, compressive sensing, waveforms, optimization

1. INTRODUCTION

Compressive sensing (CS) provides a new paradigm in data acquisition and signal processing in radar, based on the assumptions of sparsity of the unknown signal and the incoherence the transmitted waveform. The recovery of signals is possible from a reduced number of measurements because of the sparsity. Several works investigate CS radar but without taking into account the effect of the radio frequency (RF) system components on the incoherence of the received signal [1, 2]. Moreover, most works are concentrated on the use of random signal acquisition rather than deterministic, which increases the complexity of the hardware. In this work, we investigate which deterministic waveform(s) would be optimal in CS radar, based on their incoherence, as well as the RF transmission and reception constraints, e.g., required bandwidth B_f to match the initial incoherence and ease of generation, transmission and reception. We illustrate this for the basic radar case of range-only estimation.

In Section 2, we introduce our data model along with the requirements for CS radar. Several deterministic waveforms with good autocorrelation properties are presented in Section 3, where we discuss their feasibility in CS radar. In Section 4, the RF system is presented and sparse signal recovery (SSR) is introduced. Section 5 and Section 6, overview our findings on the optimization of the incoherence of the waveforms, and our simulation results. Conclusions are drawn in Section 7.

2. CS RADAR DATA MODEL

Assume a monostatic radar setup, where the measurements $\mathbf{y} = \mathbf{r} + \mathbf{e}$ at the receiver are modeled as the radar echoes $\mathbf{r}$ in Gaussian noise $\mathbf{e}$. If we consider a radar scene $\mathbf{x}$, containing only ranges, then the received echo $\mathbf{r}$ in CS is given by the linear model

$$\mathbf{r} = \mathbf{S}\mathbf{x}, \tag{1}$$

where $\mathbf{r}$ contains the contributions of all targets and $\mathbf{S}$ is the sensing matrix. Each entry of $\mathbf{x}$ occupies a range cell with size $\Delta\tau = 1/f_s$, where $f_s = 1$ is the reference sampling frequency of $s(t)$. $\mathbf{S}$ has Toeplitz structure i.e., its columns are shifted copies of $s[n] = s(n/f_s)$, $n = 0, 1, \ldots, L-1$:

$$\mathbf{S} = \begin{bmatrix} s[0] & \cdots & 0 \\ \vdots & \ddots & \\ s[L-1] & & s[0] \\ & \ddots & \vdots \\ 0 & \cdots & s[L-1] \end{bmatrix}_{(N+L)\times N}. \tag{2}$$

Each shift , $k = 0, 1, \ldots, N-1$, in (2), corresponds to a time delay $\tau_k = k/f_s$, and is related to the target range. The range profile $\mathbf{x}$ can be assumed sparse, having only $K < N$ significant components, where K is the number of targets.

2.1. Incoherence and autocorrelation

The fundamental measure of the quality of a radar waveform is the ambiguity function (AF), which usually is a two-dimensional representation of the cross-correlation of the waveform with its shifted copies in time and Doppler. For zero-Doppler, the AF is equivalent to the aperiodic autocorrelation function (ACF) of the signal $s[n]$:

$$\mathcal{A}[k] = \frac{1}{L}\sum_{n=0}^{L-1-k} s[n]s^*[n-k],\ k = 0, 1, \ldots, N-1. \tag{3}$$

With CS, the unknown signal $\mathbf{x}$ can be recovered, under the conditions that $\mathbf{x}$ is sparse, and the measurement matrix $\mathbf{S}$ is "sufficiently" incoherent [3]. The incoherence is essential for the reconstruction algorithms and the number of measurements to be taken [3]. There are several measures for the

coherence of a matrix: the mutual coherence, the restricted isometry property (RIP) and the null-space-property (NSP), with the last two being more difficult to calculate.

The mutual coherence of a matrix $\mathbf{S}$ is given by the largest inner product of the columns of $\mathbf{S}$, denoted $\mathbf{s}_k, k = 1, 2, \ldots, N$ and normalized, i.e. $||\mathbf{s}_k||_2 = 1$:

$$\mu(\mathbf{S}) = \max_{i \neq k} |\langle \mathbf{s}_i, \mathbf{s}_k \rangle|. \quad (4)$$

Assuming $\mathbf{S}$ as in (2), there is clearly a connection between $\mu(\mathbf{S})$ from (4) and the ACF of the waveform from (3). The mutual coherence can be viewed as the largest off-diagonal value of $\mathbf{S}^H\mathbf{S}$, where $(\cdot)^H$ denotes Hermitian transpose. Furthermore, due to the Toeplitz structure of $\mathbf{S}$, the mutual coherence $\mu(\mathbf{S})$ is related to the ACF. Each column of $\mathbf{S}^H\mathbf{S}$ is the ACF of $\mathbf{s}_k$ at a certain delay τ_k. In the context of radar, $\mu(\mathbf{S})$ is the highest sidelobe in the ACF.

3. OPTIMAL WAVEFORMS

Conventional pulse radar would transmit a linear frequency modulated (LFM) pulse $s[n], n = 0, 1, \ldots, L-1$:

$$s[n] = e^{\frac{j\pi n^2 B_s}{L}}/\sqrt{L}, \quad (5)$$

where the pulse length $L = 100$ in our analysis.

The sampling frequency f_s is normalized to 1, and we choose a LFM pulse with a double sided bandwidth $B_s = 0.8$, as the reference waveform. The theoretical sidelobe level of the LFM is -13.4 dB [4].

Since the power amplifier in the radar transmitter is operated in saturation (Class C), all amplitude modulation of the waveform is unwanted, and if allowed can cause signal clipping and unwanted distortion. From the theoretically optimal waveforms with constant unit amplitude and good correlation properties (e.g. [1] and [2]), we choose two (discrete) phase sequences, namely the cubic Alltop sequence and the Björck sequence. The cubic Alltop sequence origins from a continuous phase signal, while the Björck sequence is a truly discrete binary sequence.

In [5], Alltop defines a cubic phase sequence:

$$s[n] = e^{\frac{j2\pi n^3}{L}}/\sqrt{L},\ 0 \leq n \leq L-1, \quad (6)$$

with sidelobes of $L^{-1/2}$ for the periodic ACF and sidelobes close to this value for the aperiodic case.

The Björck sequence falls in the family of CAZAC (constant amplitude zero autocorrelation) sequences and is of prime length L. The Björck sequence is known to have a zero periodic ACF and nearly zero aperiodic ACF with uniformly low sidelobes [2]:

$$s[n] = e^{j2\pi\left[\left(\frac{n}{L}\right)\right]\arccos\left(\frac{1}{1+\sqrt{L}}\right)}/\sqrt{L},\ 0 \leq n \leq L-1, \quad (7)$$

where $L \equiv 1 (\mathrm{mod}\ 4)$ prime and $\left[\left(\frac{n}{L}\right)\right]$ the Legendre symbol, and taking values ± 1.

The cubic Alltop and Björck sequence are promising for CS radar implementation, as their correlation sidelobes are flat, with no particular sidelobe structure. The ACFs are shown in Fig. 1, where the clear advantage of a narrower mainlobe over the conventional LFM is notable.

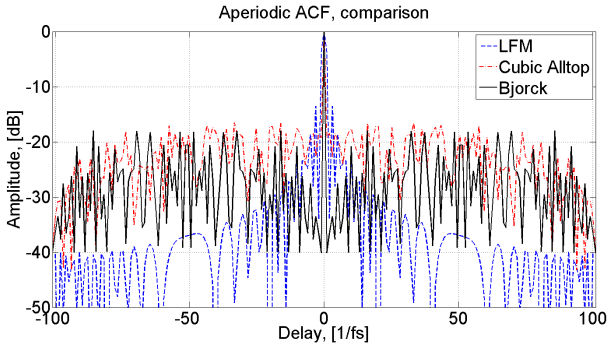

Fig. 1. ACF - Linear chirp, cubic Alltop and Björck.

4. RF SYSTEM

We model the radar system as a general digital RF system as shown in Fig. 2. A typical realization of such a system will require a fast DAC, ADC and a DDC (digital down converter). We concentrate on the digital band-pass filters (BPFs) and Hilbert transform. The power amplifiers and the analog filters are not included at this point.

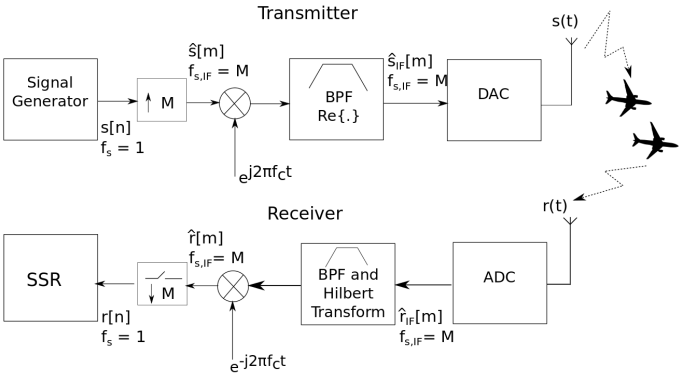

Fig. 2. Simplified block scheme of a generalized RF transmitter and receiver

After the initial sequences are generated at rate $f_s = 1$ they are interpolated to a new sequence $\hat{s}[m]$, at rate $f_{s,IF} = M$, in order to allow for digital up-conversion to intermediate frequency (IF). The initial Alltop sequence is linearly interpolated $\hat{s}[m] = (s[\lfloor m/M \rfloor + 1] - s[\lfloor m/M \rfloor])(m \bmod M)/M + s[\lfloor m/M \rfloor]$ and the binary Björck is put on a rectangular pulse shape $\hat{s}[m] = s[\lfloor m/M \rfloor]$ in order to keep it binary , where

$m = 0, 1, \ldots, ML-1$, $n = 0, 1, \ldots, L-1$ and $\lfloor \cdot \rfloor$ denotes the floor function. After the up-conversion the resultant signal is filtered to constrain its bandwidth and to filter any harmonics from the mixing.

The receiver basically does the inverse of the transmitter, starting with ADC which samples $r(t)$ at rate $f_{s,IF} = M$. We use Hilbert transform to recover the complex signal and another low-pass filter (LPF) which precedes the final down-sampling to the reference rate $f_s = 1$.

The double sided bandwidth B_f of all filters is tunable and relative to the reference sampling frequency $f_s = 1$.

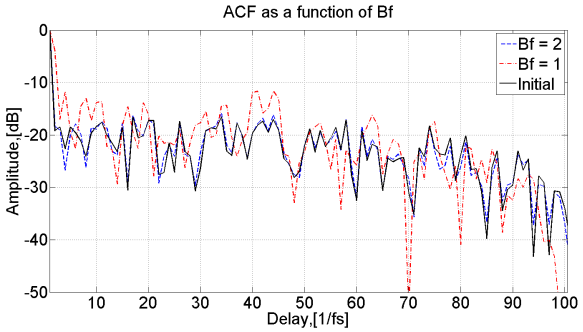

Fig. 3. Aperiodic ACF of a cubic Alltop sequence as a function of the double sided filter bandwidth B_f.

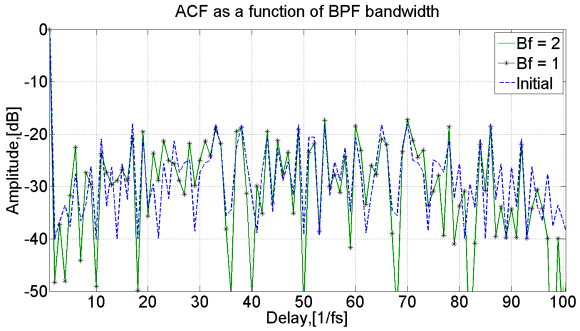

Fig. 4. ACF of a Björck seqence as a function of double sided filter bandwidth B_f.

4.1. Sparse signal recovery (SSR)

In traditional radar processing, the matched filter (MF):

$$\mathbf{x}_{\text{MF}} = \mathbf{S}^H \mathbf{y} \tag{8}$$

is the optimal test statistics for a likelihood based detection and estimation.

Several SSR methods [6] are available for implementation in CS radar. We prefer a Bayesian approach, implemented as a complex fast Laplace (CFL) algorithm because it is robust to noise and is executed in nearly real time (FL from [7] adapted for complex signals in [8]). The Bayesian approach leads to an SSR estimator:

$$\mathbf{x}_{\text{SSR}} = \arg\min_{\mathbf{x}} \{|\mathbf{y} - \mathbf{S}\mathbf{x}|^2 + \lambda ||\mathbf{x}||_1\}, \tag{9}$$

where the parameter λ balances between the noise energy and the sparsity.

5. OPTIMIZATION OF THE ACF

Although already good, it is worth trying to optimize the ACF of the waveforms even further. The problem of optimization of the ACF of a sequence is comparable to minimizing the Frobenius norm:

$$\min ||\mathbf{S}^H \mathbf{S} - \mathbf{I}||_F^2, \tag{10}$$

where $\mathbf{I}$ is an identity matrix, $\mathbf{S}$ is Toeplitz and given by (2). The problem of designing unimodular sequences with low correlation has already been studied, and a particular algorithms for dictionary optimization are provided in [9, 10]. Due to the high complexity of solving the quadratic function (10), both algorithms tackle the problem of minimizing the average coherence of $\mathbf{S}$ which is given by the integrated sidelobe level (ISL) [9, 10] of the ACF:

$$\text{ISL} = \sum_{k=1}^{L-1} |\mathcal{A}[k]|^2. \tag{11}$$

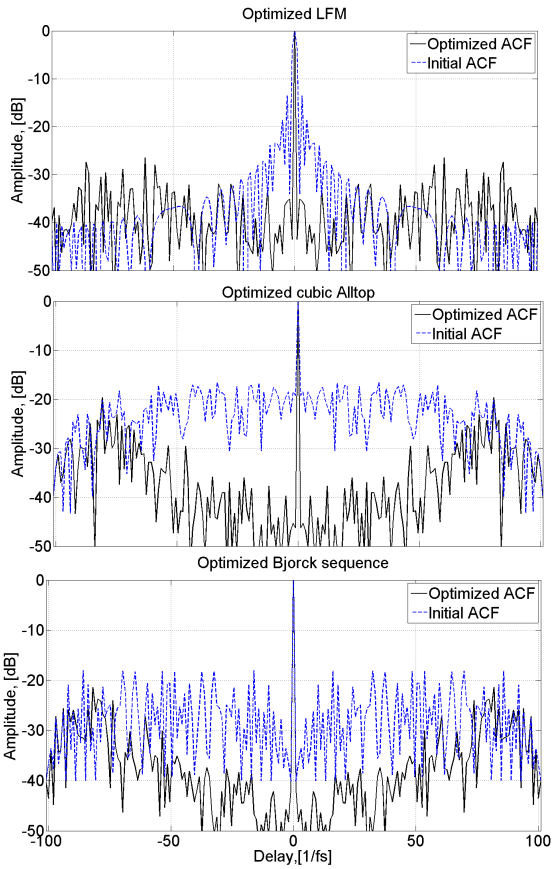

Fig. 5. Optimized waveforms

We use the CAP (cyclic algorithm - pruned) method presented in [10], since it shows to preserve both the structure of the $\mathbf{S}$ matrix and the *general* phase behavior of the initializing sequence.

6. RESULTS

6.1. RF band pass filter effects

The effect of the RF system on the ACF of the optimal waveforms defined in Section 3 is investigated in this subsection.

An LFM with $L = 100$, and Alltop and Björck with $L = 101$ are analyzed. We start with $B_f = 1$ for the cubic Alltop and we observe an increase of the sidelobes of about 4 dB. Additionally, the main lobe is wider due to the filtered high frequency components of the waveform, as shown in Fig. 3. By increasing $B_f = 2$, the ACF of the received cubic Alltop matches the initial one well.

For the Björck sequence the required B_f for good reception, e.g., without increase of the sidelobe level, is $B_f = 1$ as shown in Fig. 4, since the transmitted binary sequence can be recovered at the receiver.

6.2. Optimization results

Here, we present some results of the optimization algorithm from Section 5. Optimization of the initial waveforms by means of minimizing the ISL as in (11), clearly results in a decrease of the sidelobes as shown in Fig. 5. The sinc function structure of the autocorrelation of the LFM is lost and additionally there is a decrease in the width of the main lobe. For the optimized cubic Alltop and Björck the sharp response at zero delay is contained and a couple of dBs are gained in the sidelobe level.

6.3. Sparse recovery

In Section 6.1 we showed that with properly selected B_f the received waveform does not experience increase in the ACF sidelobes. In this section, we are showing the performance of the initial waveforms through SSR and MF, without taking into account the effects of the RF system.

We are showing a comparison between $\mathbf{x}_{\text{MF}}$ in (8) and $\mathbf{x}_{\text{SSR}}$ in (9), approximated by the CFL. For a threshold, as in [11], with a probability of false alarm $P_{FA} = 10^{-6}$, we present a comparison between the performance of the different waveforms. The SNR is defined per target.

The weak target cannot be distinguished from the noise or the sidelobes in the conventional MF based detection. In such a case the SSR is an improvement of the MF since it uses the entire contribution of the ACF instead of just the MF peaks above a predefined threshold, as shown in Fig. 6.

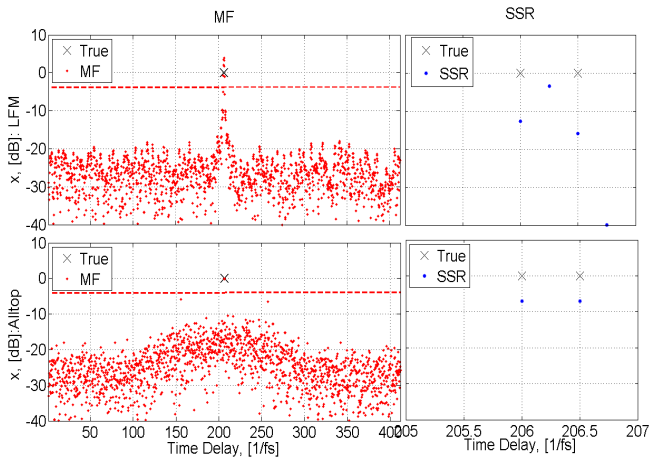

Fig. 7. Recovery of two targets (16 dB) in noise separated by 1/2 reference cell, averaged over 10 noise realizations and normalized by the target SNR. The dashed red lines indicate the MF threshold (at $P_{FA} = 10^{-6}$).

The cubic Alltop sequence is compared to the LFM in a high resolution test ($\Delta\tau = 1/(Qf_s), Q = 4$), where $\mathbf{S}$ is constructed as a $(N + L - 1) \times NQ$ matrix with the $(n, k)^{\text{th}}$ element given by:

$$s(n/f_s - k/(Qf_s)), \tag{12}$$

where $s(t)$ is transmitted in the time interval $[0, L/f_s)$, $n = 0, 1, \ldots N + L - 1$, and $k = 0, 1, \ldots, QN - 1$. In such a case, $\mathbf{S}$ has a block Toeplitz structure and the system in (1) is under-determined.

In Fig.7 we present a zoomed plot around the targets. No contributions are present in other regions of the radar scene. The Alltop sequence outperforms the LFM, as shown in Fig. 7, due to the wider mainlobe of the LFM. Furthermore, the specific sinc structure in the ACF of the LFM results in confusion between the main lobe contribution and some of the sidelobes, and the two targets cannot be resolved as shown in Fig. 7.

7. CONCLUSIONS

The proper choice of waveform is essential in CS radar. In this work, we showed that the mutual coherence of the measurement matrix $\mathbf{S}$ is related to the ACF of the transmitted waveform, due to the specific structure in $\mathbf{S}$. We investigated several deterministic waveforms which show optimal behavior in CS radar taking into consideration not only the waveform properties itself, but also the effect of BPF width B_f in the RF system. We showed that the cubic Alltop sequence requires a wider bandpass filters ($B_f \approx 2$) so that no increase of the sidelobes appears. The Björck sequence can be transmitted on a rectangular pulse shape and recovered with a filter of $B_f = 1$. The coherence of the investigated waveforms can be

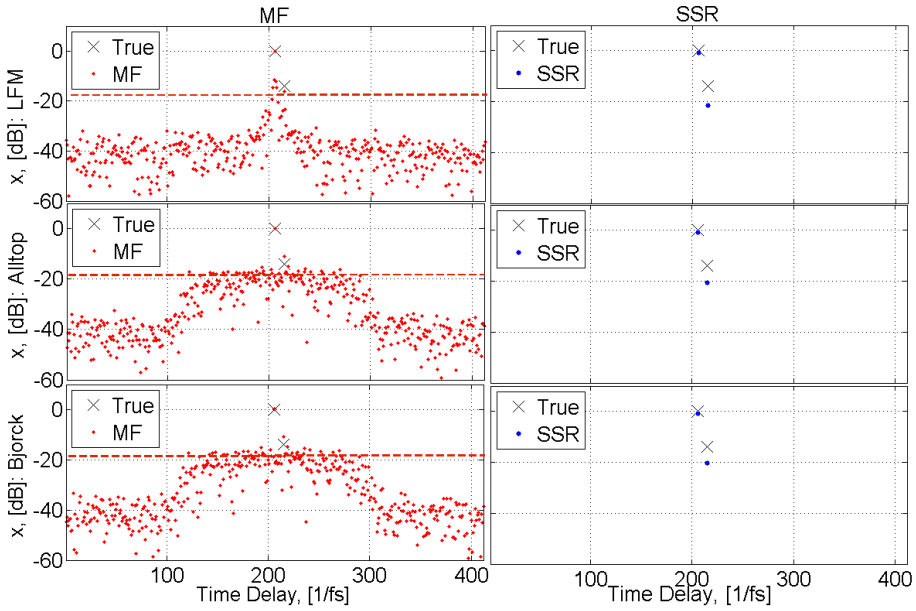

Fig. 6. Recovery of two targets in noise (SNR = 30 dB and SNR = 16 dB), separated by 10 range cells and averaged over 10 noise realizations; normalized by the strongest target SNR. The dashed red lines indicate the MF threshold (at $P_{FA} = 10^{-6}$).

reduced even further with an optimization algorithm, which minimizes the average coherence, given by the ISL metric.

SSR allows resolving weak targets (even as weak as the sidelobes of the ACF) with a proper selection of the transmitted waveform, and threshold for a given P_{FA}. Despite the larger required transmission bandwidth B_f, our preference for an optimal waveform is the cubic Alltop sequence, because it outperforms the conventional LFM pulse in resolution, and is more flexible than the Björck sequence to generate in terms of length (no requirement for prime length).

In future work, the behavior of the optimized waveforms will be investigated further through the transmission-reception chain. Furthermore, the reconstruction performance will be investigated under compression of the received data, and a bound for the number of required measurements for a given number of targets will be derived.

8. REFERENCES

[1] M.A. Herman and T. Strohmer. High-resolution radar via compressed sensing. *IEEE Transactions on Signal Processing*, 57(6):2275 –2284, June 2009.

[2] A. Kebo, I. Konstantinidis, J.J. Benedetto, M.R. Dellomo, and J.M. Sieracki. Ambiguity and sidelobe behavior of CAZAC coded waveforms. In *2007 IEEE Radar Conference*, pages 99 –103, April 2007.

[3] E.J. Candes, J. Romberg, and T. Tao. Robust uncertainty principles: exact signal reconstruction from highly incomplete frequency information. *Information Theory, IEEE Transactions on*, 52(2):489 – 509, feb. 2006.

[4] C.E. Cook and M. Bernfeld. *Radar Signals: An Introduction to Theory and Application*. Artech House Radar Library. Artech House, 1993.

[5] W. Alltop. Complex sequences with low periodic correlations (Corresp.). *IEEE Transactions on Information Theory*, 26(3):350 – 354, May 1980.

[6] J.A. Tropp and S.J. Wright. Computational methods for sparse solution of linear inverse problems. *Proceedings of the IEEE*, 98(6):948 –958, june 2010.

[7] S.D. Babacan, R. Molina, and A.K. Katsaggelos. Bayesian compressive sensing using laplace priors. *Image Processing, IEEE Transactions on*, 19(1):53–63, Jan. 2010.

[8] R. Pribic and H. Flisijn. Back to Bayes-ics in radar: Advantages for sparse-signal recovery. *COSERA*, May 2012.

[9] M. Elad. Optimized projections for compressed sensing. *IEEE Transactions on Signal Processing*, 55(12):5695 – 5702, December 2007.

[10] P. Stoica, Hao He, and Jian Li. New algorithms for designing unimodular sequences with good correlation properties. *IEEE Transactions on Signal Processing*, 57(4):1415 –1425, April 2009.

[11] J.J. Fuchs. *The Generalized Likelihood Ratio Test and the Sparse Representations Approach*, volume 6134 of *Lecture Notes in Computer Science*. Springer Berlin Heidelberg, 2010.